Journal Pre-proofs

Characterization and anti-tumor bioactivity of astragalus polysaccharides by immunomodulation

Wenfang Li, Xueyan Hu, Shuping Wang, Zeren Jiao, Tongyi Sun, Tianqing Liu, Kedong Song

Please cite this article as: W. Li, X. Hu, S. Wang, Z. Jiao, T. Sun, T. Liu, K. Song, Characterization and anti-tumor bioactivity of astragalus polysaccharides by immunomodulation, *International Journal of Biological Macromolecules* (2019), doi: https://doi.org/10.1016/j.ijbiomac.2019.09.189

Characterization and anti-tumor bioactivity of astragalus polysaccharides by immunomodulation

Wenfang Li [a], Xueyan Hu [a], Shuping Wang [b], Zeren Jiao [c], Tongyi Sun[d], Tianqing Liu [a], Kedong Song [a],*

a State Key Laboratory of Fine Chemicals, Dalian R&D Center for Stem Cell and Tissue Engineering, Dalian University of Technology, Dalian 116024, China;
b Chemical Engineering, Dalian University of Technology, Dalian 116024, China;
c Artie McFerrin Department of Chemical Engineering, Texas A&M University, College Station, Texas, USA;
d School of Biological Science and Technology, Weifang Medical University, Weifang 261042, China;

*Corresponding author Tel.: +86-411-84706360
E-mail address: Kedongsong@dlut.edu.cn

Keywords: Astragalus polysaccharide; Macrophages activation; Cell apoptosis; Mitochondria pathway; Immunoregulation

Abstract

Astragalus polysaccharide (APS) has attracted growing interests in the field of anti-cancer by direct killing effect and improving immune function. In this study, the structure and composition of APS was determined, following the evaluation of *in vitro* and *in vivo* anti-tumor activity of APS targeted macrophages and host immune system based on immunoregulated strategy. The results indicated that APS had no direct cytotoxicity against 4T1 cells, but APS mediated macrophages could significantly inhibit the growth of 4T1 cells by the induction of cell cycle arrest (G2 phase) and cell apoptosis. APS mediated macrophages promoted the apoptosis of 4T1 cells mainly through the mitochondrial apoptosis pathway. The *in vivo* findings demonstrated that APS could markedly improve the thymus index and spleen index, and restore the structure of the damaged thymus and spleen tissue. APS could significantly enhance the proliferation of spleen lymphocytes and increase phagocytosis of peritoneal macrophages in mice. Furthermore, APS was capable of up-regulating the expression of IL-2, TNF-α and IFN-γ in peripheral blood. APS combined with 5-FU could improve the anti-tumor effect accompanied by the immunosuppressive alleviation of 5-FU on immune system, which may be suitable as an immune adjuvant for chemotherapy.

1. Introduction

Breast cancer is a leading dominant cause of cancer death in women worldwide. Chemotherapy is acknowledged as one of the most effective strategies for multiple cancers [1]. However, many drawbacks induced by chemotherapy drugs remain challenge including immunosuppression, multiple organic toxicities as well as multidrug resistance. Therefore, it is urgent to develop supplementary anti-tumor agents with better therapeutic effectiveness and less toxicity in the treatment of breast cancer.

Increasing evidences have demonstrated that polysaccharides from natural resources (plants, animals and fungi) may provide promising strategy in the prevention or treatment of cancer [2, 3].The most typical representative polysaccharides are lentinan, schizophyllan and polysaccharopeptide which have been widely used as the adjuvant drugs for cancer therapy in domestic and foreign market [4]. The anti-tumor bioactivity of polysaccharides is achieved through direct tumor killing, the enhancement of immune function and synergistic chemotherapy [5, 6]. Astragalus polysaccharide (APS), one of the active constituents of astragalus membranaceus, has been proved to have broad-range biological activities especially its tumor-killing effect. Yu et al demonstrated that APS showed direct apoptosis-induced effects on MGC-803 cells via cell cycle arrest and mitochondrial apoptosis pathway [7]. Most clinical trials and animal studies indicated that APS displayed indirect cytotoxicity towards tumor cells or used in combination strategy with chemotherapy drugs by improving host immune response [8, 9].

In our previous study, it was found that APS itself failed to inhibit the growth MCF-7 cells, but APS exhibited cytotoxicity of the supernatant of RAW264.7 cells on MCF-7 cells via the Toll-like receptor 4 (TLR4)-mediated up-regulation of tumor necrosis factor-α (TNF-α) and nitric oxide (NO). In other words, the anti-tumor activity of APS was associated with the immunoregulating effects on macrophages [10]. Although it was convenient to study the *in vitro* effect and mechanism of APS mediated macrophages on breast cancer cells, the anti-tumor activity of the single immune cell was far different from that of *in vivo* immune system. Therefore, we further investigated the *in vivo* anti-breast cancer effect of APS in BALB/c mice from the immune organs, immune cells and cytokine secretion. In this study, we investigated the *in vitro* and *in vivo* anti-tumor activity of APS from immunomodulation for the first time, which aimed to provide more experimental bases for the clinical application of APS and its adjunctive therapy in anti-breast cancer.

2. Methods

3

2.1. Materials and reagents

RAW264.7 and 4T1 cells were purchased from Zhongqiao Xinzhou Biotechnology Co. Ltd. (Shanghai, China). The medium was changed every 2 days. Passage was needed when cells reached 80-90% confluence. APS was purchased from Pharmagenesis Inc. (Beijing, China). 5-fluorouracil (5-FU) was obtained from Sigma Aldrich Co. (St Louis, MO, USA). RPMI-1640 medium and fetal bovine serum (FBS) was purchased from Gibco Co. (Carlsbad, CA, USA). Calcein-AM, propidium iodide (PI) and Hoechst 33342 were obtained from Calbiochem (San Diego, CA). Cell counting kit-8 (CCK-8) was obtained from Selleck.cn (Shanghai, China). Cell cycle analysis, Annexin V-FITC apoptosis kits were purchased from Beyotime Institute of Biotechnology (Haimen, China). Anti-Bcl-2 antibody anti-Bax antibody was purchased from Abcam Inc. (Cambridge, MA, USA). Mouse TNF-α, IL-2 and IFN-γ ELISA kits were purchased from Boster Biological Technology Co. (Wuhan, China).

2.2. Chemical characterization of APS

A field emission scanning electron microscope (SEM, NanoSEM 450, FEI, USA) was used to investigate the microstructure of APS. APS powders were fixed on the conductive adhesive and sputtered with gold, followed by observation with different magnifications. Nuclear magnetic resonance (NMR) was conducted to evaluate the configuration of glycoside bond and anomeric carbon of APS. A total of 30mg APS was dissolved in 0.5 mL of D_2O in a NMR tube. ^{1}H-NMR and ^{13}C-NMR spectra were recorded on a Bruker AVANCE III 500 MHz Digital NMR spectrometer (Bruker, Switzerland). Monosaccharides composition of APS was analyzed by reverse-phase high performance liquid chromatography (HPLC) as previously described [11]. HPLC assay was performed on a WondasilTM-C18 column (4.6 mm i.d. × 150 mm, 5 μm, Shimadzu, Japan) at 35 °C. The mobile phase A and B was 0.1 mol/L phosphate (pH=6.9) buffer and acetonitrile with a volume ratio of 82:18. The injection volume was 20 μL. Elution was conducted at a flow rate of 1.0 mL/min.

2.3. Effect of APS and APS-mediated macrophage supernatant on 4T1 cells
2.3.1. Collection of condition medium

APS was dissolved in DMEM at different concentrations (50, 100, 200, 500, and 1000 μg/mL, respectively) and filter-sterilized with the 0.22 μm membrane filter. RAW264.7 cells (1×10^5 cell/mL) were seeded in 24-well plates and incubated with various concentrations of APS

4

solution for 24 hours. The supernatants of each group were collected, followed by centrifugation at 3000 rpm for 10 min. Here, the supernatants of macrophages with different concentrations of APS were collected and referred as conditioned medium (CM) and stored at -20 °C for later use.

2.3.2. Effects of APS and CM on cell growth and proliferation

Live/Dead staining and CCK-8 assay were used to evaluate the effect of APS and CM on the growth of 4T1 cells. Briefly, 4T1 cells ($2×10^4$ cells/mL) at logarithmic growth phase were seeded in 96-well plates. After overnight, the original medium was removed, various concentrations of APS (50, 100, 200, 500, 1000 μg/mL) and CM solutions were added. RPMI-1640 complete medium and 5-FU solution (50μg/mL) were used as negative and positive controls, respectively. After incubation of 72h, cells were subjected to Calcein-AM (2 μmol/L of), PI (4 μmol/L of) and of Hoechst 33342 (5 μg/L) and incubated in a 37 °C incubator for 15 min. Subsequently, cells were observed and photographed under a fluorescence microscope (IX83, Olympus, Japan). For CCK-8 assay, cell culture and treatment with APS and CM were conducted as above. At each time point of 24h, 48h and 72h, APS-containing medium and CM in each well was replaced by 10 μL of CCK-8 solution and 100 μL of RPMI-1640 medium. Then cells were incubated in the dark at 37 °C for 3h. The absorbance values in each group were measured at 450 nm using microplate reader (Varioskan Flash, Thermo Fisher Scientific, San Jose, CA, USA).

2.3.3. DAPI staining

DAPI staining was conducted to identify the changes of chromatin induced by serial concentrations of APS and CM solution. 4T1 cells ($2×10^4$/mL) were seeded in 24-well plates with 1 mL complete medium per well. After cell attachment, different concentrations of APS and CM solution were added. Complete medium and 5-FU solution were used as negative and positive control groups, respectively. After 48h incubation, cells were fixed with 4% paraformaldehyde for 30 min and incubated with DAPI at 37 °C for 20min. The nuclear morphologies of treated cells were observed and photographed under a fluorescence microscope.

2.3.4. SEM assay

Cells were seeded in the coverslips in 24-well plates. The processes of cell treatment with APS and CM were the same as DAPI staining. After 48 hours incubation, cells were fixed with 2.5% glutaraldehyde for 3 hours, followed by dehydration of increasing concentrations of ethanol (50%, 70%, 90%, and 100%, v/v) and dried at room temperature. Cells morphologies were observed with SEM with accelerating voltage of 30.0 kV and exposure time of 6 μs after being sprayed with gold for 90s.

2.3.5. Cell cycle

Cell cycle was performed as previously described [12]. Briefly, 4T1 cells ($1×10^6$ cells/mL) were seeded in 6-well plates and subjected to CM mediated by various concentrations of APS. After 48h of incubation, cells were routinely digested with trypsin and collected followed by wash with cold PBS. Then cells were fixed with 70% ethanol at 4°C overnight and treated with 100 μg/mL RNase solution and PI staining at 37°C for 30 min. The samples were detected at the wavelength of 488 nm using a flow cytometer (FACS Canto, BD Biosciences, USA), and the relative proportions of 4T1 cells in each phases were analyzed with Modfit software (Verity Software House Inc., Topsham, ME, USA).

2.3.6. Annexin V-FITC/PI detection

The extent of cell apoptosis was assayed using Annexin Ⅴ‑FITC‑PI apoptosis kit. 4T1 cells ($1×10^6$ cells/mL) were seeded in 6-well plates and treated with CM for 48h. Cells were collected following digestion with EDTA-free trypsin, wash with PBS and centrifugation for 5min at 1000rpm. Subsequently, cells were subjected to 5 μL of Annexin V-FITC and 5 μL of PI were added and incubated at room temperature in the dark for 10min. Cells were then filtered through a 40 μm cell filter and tested by flow cytometry.

2.3.7. Expression of apoptotic proteins and cytochrome

Immunofluorescence and flow cytometry assays were used to assess the effect of CM on the expression of apoptosis-related proteins in 4T1 cells. After 48 h of culture, cells were fixed with 4% paraformaldehyde for 20 min, permeabilized at 0.2% Triton X-100 for 20 min at room temperature and then blocked with 5% bovine serum albumin (BSA) in PBS for 30 min. Then cells were subjected to the primary antibody of Bcl-2, Bax and cytochrome C (rabbit anti-mouse, 1:100) and incubated overnight at 4 °C. After the removal of primary antibodies, cells were incubated with Dylight 549 conjugated goat anti-rabbit antibody (1:50) at room temperature for 60min. The nuclei of 4T1 cells were counterstained with DAPI at 37°C for 15 min, and photographed under a laser confocal microscope (FV1000, Olympus, Japan). In addition, the expressions of Bcl-2 and Bax were quantitatively analyzed using flow cytometry after exposure to CM for 48h as previously described [13].

2.3.8. Activity changes of caspase-9 and caspase-3

After 48h of incubation with CM, 4T1 cells were collected and treated with lysis buffer in ice bath for 15min. Then cells were centrifuged at 10,000 rpm for 15 min. The supernatant was collected and pre-cooled in ice bath. A total of 50 μL cell lysate supernatant was mixed with 40

μL detection buffer, followed by addition of 10μL corresponding catalytic substrate Ac-LEHD-pNA (2mM) and Ac-DEVD-pNA, respectively. The absorbance value of each well was measured at 405 nm. The pNA content in each group was calculated according to the obtained standard curve.

2.4. Mouse breast cancer model and treatment protocol

All animal studies were performed in accordance with the regulatory guidelines for the care and use of laboratory animals and were approved by Ethics Committee of Dalian Medical University. Ninety BALB/c mice (approximately 6~8 week-old, female) were purchased from Dalian Medical University. All mice were housed in a sterile environment under controlled temperature and humidity with a 12 h light/dark cycle. A total of 100 μL 4T1 cells (1.5×10^7cell/mL) in sterile saline were subcutaneously injected into right front forelimb of BALB/c mice except for the blank group. The length (a) and width (b) of tumor were measured with calipers every 3 days. The tumor volume was calculated as previous report [14]: $V = 1/2\ ab^2$. The tumor models with the volume of about 100 mm^3 were used for further study.

After the successful tumor modeling, all mice were randomly divided into six groups, including blank group, negative control group, APS groups (100 and 200 mg/kg), 5-FU group (20 mg/kg) and combined group (200mg/kg APS+20mg/kg 5-FU). The mice in blank and negative control groups were injected intraperitoneally with 0.9% normal saline, while APS groups were injected intraperitoneally with APS solution at the dose of 100 mg/kg and 200 mg/kg. All mice were successively administrated with the above drugs for 14 days. Mice took food and water freely in experimental period.

2.5. Calculation of tumor inhibition rate and immune indices

The behavior, diet, reaction and death of the mice after administration were observed during experimental period. The body weights of the mice were recorded every other day. The length and width of the tumors were measured every 2 days, and the tumor volumes were calculated. After 24 hours of final administration, parts of the mice were drawn blood from eyeball and were sacrificed by cervical dislocation. The tumors, thymuses and spleens were immediately excised and weighed. The *in vivo* tumor inhibition rate was calculated as: Tumor inhibition rate (%) = [1 − (average tumor weight of experimental group/ average tumor weight of model group)]

×100. The viscera indices for thymus and spleen were measured as the average weight of the viscera to the body weight (mg/g) of mice.

2.6. Pathological examination of tumor and immune tissues

The harvested tumor and immune tissues (spleens and thymuses) of all groups were fixed in 10% formalin, embedded in paraffin and cut into 5 μm sections. All tissue samples were stained with hematoxylin and eosin (H&E) to observe the histopathological changes according to routine procedure.

2.7. Neutral red uptake assay of macrophages

The phagocytosis capacity of peritoneal macrophage was assayed with neutral red solution [15]. The peritoneal macrophages were obtained from BALB/c mice (n=4) in each group which were injected intraperitoneally with 4% mercaptoethyl starch broth solution 3 days in advance. Briefly, the macrophages were treated with 5% neutral red solution for 10min and washed in PBS twice, followed by addition of cell lysis buffer (anhydrous ethanol: acetic acid = 1:1, v/v). The absorbance values of supernatant liquids were measured at 540 nm. The phagocytosis index (PI) was used to evaluate the phagocytic ability of peritoneal macrophages which referred to the ratio of the absorbance in modeling mice (all treated groups) to the absorbance in normal mice (blank group).

2.8. The proliferation activity of splenic lymphocytes

After scarification by cervical dislocation, the mice (n=4) in each group were immersed in 75% alcohol for 5 min. The spleens were collected and cut into two parts. Cells were collected by gently scraping the inside of the spleens with a sterile cover glass. Then cells were filtered with 200 mesh filter, and erythrocytes were lysed. Splenic lymphocytes ($1×10^6$ cells/mL) were seeded in 96-well plates with 100 μL per well and treated with LPS (10 μg/mL) for 48h. Then lymphocytes were subjected to 10 μL of CCK-8 solution and 100 μL of RPMI-1640 medium in the dark at 37 °C for 4h. The absorbance values were measured at 450 nm. The proliferation activity of lymphocytes in each group was the ratio of the absorbance in treated groups to the absorbance in blank group.

2.9. Analyses of serum cytokines in mice

8

After 24 hours of the final administration, the bloods were drawn from eye orbit and were centrifuged at 3500 rpm for 10 min to obtain the serum samples. The concentrations of IL-2, IFN-γ and TNF-α were assayed using ELISA kits according to the manufacturer's instructions.

2.10. Immunohistochemical analysis of apoptosis-related proteins in tumor tissues

The expressions of Bcl-2, Bax and caspase-3 in tumor tissues were assayed according to previous method [16]. The immunohistochemical (IHC) images were semi-quantitatively analyzed using the Image-Pro Plus 6.0 (IPP, Media Cybernetics, USA) software.

2.11. Statistical analysis

All data were expressed by mean ± standard deviation (Mean ± SD). All experiments were performed at least three times. Statistical analysis was performed using one-way analysis of variance (ANOVA). $P < 0.05$ was considered as significant difference. All statistical analyses were conducted using Origin 8.0 software (Origin Lab, MA, USA).

3. Results and discussion

3.1. Polysaccharide characterization

The physicochemical and structural features of polysaccharides are directly responsible for their biological activities [17, 18]. Accumulating evidence have demonstrated that polysaccharides with the structure of (1→3) or (1→4)-β-D-glucan appear to have better anti-cancer or immunopotentiating activity [19, 20]. The structure features and concomitant bioactivities of polysaccharides differ greatly due to their different raw materials or purification processes [21]. In this study, the same batch of APS from Pharmagenesis Inc. was used to avoid possible variety in the biological activity. APS was obtained from the root of Astragalus membranaceus following by hot water extraction, gradient ethanol precipitation, column chromatography separation, ultrafiltration and microfiltration. The previous report in our lab demonstrated the high purity of APS with the absence of protein and nucleic acid. APS stacked together with spherical-like shape and nanometer sizes [10], which was also clearly shown in Fig.1A. Previous study indicated that nanostructured particles could not only passively interact with cells, but also actively mediate molecular processes and cell responses [22]. Here, the nanoscale microstructures of APS may be closely associated with the subsequent activation of macrophages.

9

The structural characteristics of APS were further confirmed with ^{1}H and ^{13}C NMR spectral analysis (Fig. 1B). The ^{1}H NMR spectra showed that the anometic protons resonances were over 4.95 ppm (δ5.017 ppm, δ5.082 ppm, δ5.110 ppm, δ5.331 ppm), suggesting the presence of α-pyranose [23], which was consistent with the glycosidic linkage types determined by IR in the previous study [10]. The peak of APS at δ4.699 ppm was attributed to the chemical shifts of deuterium oxide from D_2O. In terms of ^{13}C NMR spectra of APS, the anomeric carbon signals of APS at 99.594 ppm could be assigned to the glycosidic bonds of α-(1→6) or α-(1→4) glucan. The ^{13}C chemical signals from 70 ppm to 75 ppm corresponded to the C2 to C5 groups of α-D-glucose. The signals of C4 shifted from δ70.4 ppm to δ76.724ppm revealed the existence of (1→4) glucan. The monosaccharide compositions of APS were determined using HPLC analysis. The results indicated that APS was composed of rhamnose (Rha), galacturonic acid (GalTA), glucose (Glc), galactose (Gal) and arabinose (Ara) (Fig. 1C), which was in agreement with the results of the ^{1}H-NMR analysis of the presence of five anomeric proton signals. As reported, APS was generally known as a kind of acidic heteropolysaccharides which mainly composed of glucose, galactose, rhamnose, arabinose, xylose, fucose, fructose, mannose, ribose, glucuronic acid and galacturonic acid [24, 25], among which glucose, galactose, mannose, arabinose were the most common monosaccharides in APS [26]. It was found that polysaccharides with arabinose, rhamnose and galactose had preferable biological activity, which could significantly stimulate macrophages to secrete NO and many cytokines, and improve the immunity of the host body [27]. In this study, three monosaccharides of APS may also play an important role in the activation of macrophages *in vitro* and the *in vivo* regulation of immune systems.

3.2. Effect of APS and CM on the growth of 4T1 cells

Currently, APS has attracted growing interests in its bioactivities of anticancer and immunoregulation [28, 29]. The anti-tumor mechanism of most polysaccharides mainly includes direct killing effect and indirect anti-tumor activity by improving immune function. Previous study in our lab demonstrated that APS itself was non-cytotoxic but it significantly improved the cytotoxicity of the supernatant of RAW264.7 cells against MCF-7 cells, which may be associated with the up-regulation of TNF-α and NO induced by the RAW264.7 cells stimulation after the binding of APS and TLR4 on the surface of RAW264.7 cells [10]. In this study, we further evaluated the anti-breast cancer activity of APS *in vitro* and *in vivo* based on 2D culture and animal models.

10

As was expected, APS also failed to inhibit the growth of 4T1 cells, evidenced by the undiminished number of living cells stained by Calcein-AM and unraised dead cells stained by PI in all APS groups compared with that in untreated control group (Fig. S1A). Besides, CCK results confirmed the non-cytotoxicity of APS towards 4T1 cells (Fig. S1B). No significant differences of the numbers of living cells were noticed in APS groups compared with that in negative group, while 4T1 cells number was significantly decreased in 5-FU group compared with those in negative and APS groups (P < 0.001).

The *in vivo* studies have demonstrated that APS can inhibit tumor development via improving immunity by activating various immune cells. Among the components of the immune system, macrophages are of paramount importance in the response of innate immunity to cancer cells by releasing NO or cytokines [25, 30]. In our previous study, we confirmed that the cytotoxic effect of APS towards MCF-7 cells was associated with its immunomodulating activity on macrophages with the secretion of NO and TNF-α [10]. Here, live/dead staining and CCK assay indicated that APS mediated macrophages (CM) was cytotoxicity towards 4T1 cells. As shown in Fig.2A, the number of living cells labeled with Calcein-AM gradually decreased, and the number of dead cells with strong red fluorescence of PI increased after treatment with CM mediated with various concentrations of APS (100, 200, 500 and 1000μg/mL) for 48h. The morphology of 4T1 cells markedly changed accompanied by condensed nuclei after Hoechst 33342 staining. In addition, the results of CCK indicated that CM inhibited the growth of 4T1 cells in a time- and dose-dependent manner (Fig.2B). The highest inhibitory rate of CM mediated by APS at the concentration of 1000μg/mL reached 37.85%±5.94% after 3 days of culture. However, the cytotoxicity of CM to 4T1 was significantly lower than that of 5-FU group (P<0.001).

Cell cycle arrest is considered to be one of effective cancer-targeted therapies to prevent the proliferation of cancer cells [31, 32], which is also the same strategy for APS. Yu et al reported that APS4 inhibited cell growth by arresting cell cycle of MGC-803 cells in S phase [7]. Here, the distribution of 4T1 cells in different phases was determined after exposure to CM for 48h (Fig.2C-D). CM mediated by APS up-regulated 4T1 cells arrest in G2 phage in a dose-dependent manner. Compared to untreated group, APS at the concentration of 1000μg/mL mediated CM significantly increased the accumulation of 4T1 cells in G2 phase (P<0.01). CM mediated by APS (1000μg/mL) and 5-FU induced apoptotic peak with the sub-G1 fraction of 7.16±1.11% and 30.66±4.70%, respectively. The increased proportion of 4T1 cells in G2 phase indicated that CM was able to inhibit cell proliferation by disrupting G2 transition of cell cycle.

3.3. CM promoted the apoptosis of 4T1 cells

Apoptosis refereed to programmed cell death has become a valuable therapeutic target for anti-cancer agents [33, 34]. At present, massive studies have documented that targeting cell apoptosis is an efficient method of polysaccharides against cancer cells [35, 36]. Apoptotic cells are featured by cell shrinkage, plasma membrane blebbing, nuclear condensation, DNA fragmentation and apoptotic body formation [37]. In this study, the effects of CM on the apoptosis of 4T1 cells were systematically examined by various assays.

DAPI staining showed that the nuclei of 4T1 cells exhibited normal morphology and evenly light blue fluorescence in untreated group, which was also noticed in those groups after exposure to APS (100, 200, 500 and 1000μg/mL) for 48h (Fig. S2A). On the contrary, CM induced 4T1 cells apoptosis with typical apoptotic characteristics such as nuclear chromatin condensation and nuclear fragmentation after treatment with CM for 48h (Fig. 3A). Apoptotic bodies were observed in the presence of CM mediated by APS (1000μg/mL) and 5-FU.

Annexin V-FITC/PI assay was conducted to further quantify the apoptosis induced by CM on 4T1 cells using flow cytometry (Fig. 3B-C). CM significantly increased the percentages of apoptotic 4T1 cells after treatment with CM for 48h compared to that of untreated group (P<0.01). The highest apoptotic rate of 4T1 cells was 30.15±1.48% in the presence of CM mediated by APS (1000μg/mL).

The morphological changes of 4T1 cells were observed after treatment with CM for 48h with SEM. In untreated group, 4T1 cells adhered well and connected to each other with unclear boundary. The desmosome presented spiny-like shape with the attachment of tension microfilaments. No significant change of cell morphology was identified among all APS groups and untreated group (Fig. S2B). In contrast, CM-treated 4T1 cells displayed makeable morphological changes including clearer cell outline, reduced microfilament, swollen nuclei and foamed cell membrane. Besides, cell deformation was further striking with increased apoptotic bodies and cytolysis induced by CM with the increasing of concentrations of APS (Fig.3D).

3.4. CM mediated apoptosis by mitochondria pathway

Apoptosis occurs through two main pathways: the extrinsic or cytoplasmic pathway and the intrinsic or mitochondrial pathway, among which mitochondrial pathway is more common of polysaccharides mediating the apoptosis of cancer cells [38, 39]. Mitochondrial pathway is controlled by the Bcl-2 family of proteins. In response to apoptotic stimuli, pro-apoptotic family

members lead to the permeabilization of the outer mitochondrial membrane and the release of cytochrome-c. The cytochrome-c will bind to Apaf-1 and subsequently promote the activation of caspase (caspase‑9 and the effector caspase-3), which further activates the rest of the caspase cascade and lead to apoptosis [40]. Bax members acted as promoters provoke the efflux of cytochrome c release of cytochrome c, whereas Bcl-2 members acted as repressors blocking cytochrome c release. And the alteration in the balance between Bcl-2 and Bax is considered as more dependent to mediate cell apoptosis [41]. Currently, growing amount of anti-cancer drugs and polysaccharides are able to trigger cell apoptosis by up-regulating the ratio of Bax/Bcl-2 [42]. Yu et al demonstrated that APS had significant apoptosis-induced activity on MGC-803 cells achieved by the intrinsic mitochondrial pathway [7]. In this study, we found that APS failed to exhibit cytotoxicity towards 4T1 cells, but APS mediated the supernatant of RAW264.7 cells significantly inhibited the growth of 4T1 cells, which was consistent with Wei's study [43]. On this basis, we further investigated the mechanisms of CM induced cell apoptosis. The expressions of Bcl-2, Bax and cytochrome c in 4T1 cells were determined by immunofluorescence and flow cytometry analysis, as well as the enzyme activity of caspase-9 and caspase-3 by colorimetric assay after treatment with CM for 48 h. Compared to untreated group, CM mediated by APS down-regulated Bcl-2 expression and up-regulated Bax expression in a dose-dependent manner (Fig. 4A-B). Besides, CM mediated to APS (200, 500 and 1000μg/mL) upset the balance of Bax and Bcl-2, and significantly increased the ratio of Bax/Bcl-2 compared to that in untreated group ($P<0.01$), indicating the involvement of Bcl-2 family proteins of CM-induced apoptosis in 4T1 cells (Fig. 4C). CM mediated by APS led to the concentration dependent release of cytochrome c from mitochondria to cytosol evidenced by a gradual increase of fluorescence intensity of cytochrome c in (Fig. 4D). In addition, it was noticed that CM treatment up-regulated the activities of caspase-9, and -3 in the dose -dependent manner (Fig.4E). CM mediated by APS (500 and 1000μg/mL) significantly promoted the expression of caspase-9 and caspase-3 in 4T1 cells compared to those in untreated cells ($P<0.05$). These findings demonstrated that CM-induced apoptosis of 4T1 cells was at least in part mediated via the mitochondrial pathway.

3.5. Anticancer effects of APS on BALB/c mice

3.5.1. APS inhibited tumor growth in BALB/c mice

Growing evidence has demonstrated that APS was a potential anti-cancer agent, which not only displayed anti-tumor activity itself via enhancing the immunity, but also could improve the

13

chemotherapeutic efficacy and reduce the associated adverse effects [9, 44]. The body's immune system is very complex involving a variety of immune cells and their secreted cytokines. Compared to the simplex macrophages activation induced by APS, we further investigated the anti-breast cancer effect of APS in BALB/c mice from the immune organs, immune cells and cytokine secretion after we succeeded to develop the tumor model by subcutaneous seeding of 4T1 cells. Similarly, we noticed that APS suppressed tumor growth over time in BALB/c mice. As shown in Fig.5A, APS (100 and 200mg/kg) significantly decreased the tumor volumes compared with that of negative control group (P<0.05, P<0.01). Post-treatment for 14 days, the tumor weights and inhibitory rates were evaluated (Tab. 1). It was found that APS showed significant inhibitory effect on tumor growth in a dose-dependent manner. The tumor inhibitory rates of APS at 100 and 200mg/kg were 16.19±0.77% and 26.43±5.50%, respectively. 5-FU alone showed a makeable increase in inhibitory rate (43.26±5.59%) compared with those in APS groups. APS (200mg/kg) coupled to 5-FU yielded a higher inhibitory capacity (51.81±5.26%) of tumors in BALB/c mice. In addition, the anti-tumor activities after treatment with APS and 5-FU were also clearly identified from the appearance of the tumors (Fig. 5B). These findings indicated that APS appeared to enhance the anti-tumor activity of 5-FU.

Tumor tissues were examined by histological assay to further evaluate the anti-tumor effect of APS (Fig.5C). Tumor tissues exhibited an intact and clear architecture in negative control group. Tumor cells with large nuclei were closely arranged. APS treatment induced extensive disruption of tumor tissues. The necrotic regions of tumors in APS groups were remarkably extended in a dose-dependent manner. Increasing infiltration of inflammatory cells and nuclear fragmentation were noticed in the high-dose APS treated group, 5-FU and combine groups.

3.5.2. APS relieved immune organs damage in BALB/c mice

Immunosuppression appears to a major side effect of chemotherapy drugs, while it is not disturbing for natural polysaccharides. Instead, the polysaccharides suppress *in vivo* tumor growth based on their immunostimulatory activities [45, 46].Thymus and spleen are important immune organs which can directly reflect the immunity of the organism [47]. Thus, the immune organ indexes of BALB/c mice were determined to evaluate the effect of APS on the immune functions (Tab.2). Although the anticancer activity of APS was lower than that of 5-FU group, the spleen and thymus indices in APS groups were much higher than those of negative control and 5-FU group. APS (200mg/kg) significantly improved the spleen index (P<0.01) and thymus index

(P<0.05) compared with those in negative control group. The immune organ indices after treatment with APS (200mg/kg) combined with 5-FU increased compared to those of 5-FU alone, which indicated that APS alleviated the immunosuppressive effect on immune organs induced by 5-FU to some extent.

The effects of APS on the tissue structure of thymus and spleen were further investigated by pathological analysis. As shown in Fig.6A, the thymus especially the medulla was seriously damaged accompanied by the makeable decrease of medulla ratio in the negative control group. Compared with the untreated group, 5-FU further aggravated the destruction of thymus with the reduced size and unclear boundary between cortex and medulla. On the contrary, APS remarkably restored the thymus structure with regular arrangement of cells and increased proportion of lymphocyte (Fig.6B). APS coupled to 5-FU ameliorated thymus damage with recognizable boundary between cortex and medulla compared to that in 5-FU group. In addition, APS effectively protected the spleen with a more complete profile and identifiable boundary of marginal zone. Macrophages and lymphocytes were easily noticed in red and white pulp. All these results demonstrated the APS exhibited positive effects on immune organs which partially contributed to the anti-tumor activity.

3.5.3. APS improved immune cells response in BALB/c mice

The immune system has been well acknowledged as an important line of defense against tumors, among which immune cells (macrophages, lymphocytes, NK cells) are closely related to the anti-tumor immunity of host [48]. Massive studies have documented the immunoregulating activities of polysaccharides via stimulating various effector cell types [49]. In this study, we further evaluated the effects of APS on the phagocytic capacity of macrophages and lymphocyte proliferation in BALB/c mice. As shown in Fig.7A, neutral red particles were clearly identified in macrophages with dark red profile (blue box). The phagocytic capacity of macrophages was significantly lower in negative control group than that in blank group (P<0.05), suggesting the decreased immunity of BALB/c mice induced by tumor invasion. APS (200mg/kg) markedly improved the pinocytosis ability of macrophages compared to that in negative control group (P<0.01). In addition, the proliferation of spleen lymphocytes (blue box) stimulated with LPS was remarkably promoted in BALB/c mice treated with APS at 100mg/kg (P<0.01) and 200mg/kg (P<0.001) compared with that in negative control group (Fig.7B), which was in agreement with previous report [50]. The activities of peritoneal macrophages and lymphocytes in 5-FU group

significantly decreased compared to those in negative control group (P<0.01, P<0.001), while the immunosuppressive action was effectively alleviated with APS supplement. All these findings indicated that APS treatment provoked immune cell responses in 4T1-bearing mice.

3.5.4. APS up-regulated cytokines production

Extensive studies have demonstrated that polysaccharides can improve the production of cytokines which further contribute to anti-tumor defense [51, 52]. TNF-α is considered as a powerful immune mediator which can directly induce apoptosis of tumor cells [53]. IL-2 is capable of improving immunity and promoting the killing of autologous tumors [54]. IFN-γ has strong anti-tumor and anti-angiogenesis activity, which is capable of inhibiting the growth of cancer cells by regulating the expression of c-myc gene [55]. In this study, the effects of APS on the production of TNF-α, IL-2 and IFN-γ were measured to provide more information on the antitumor mechanisms in BALB/c mice. The expressions of TNF-α in APS groups were significantly higher than those in negative control group (P<0.05) and 5-FU group (P<0.01) as shown in Fig.8A. Although APS treatment up-regulated the production of IL-2, no significant difference of IL-2 expression was noticed among all groups (Fig.8B). Compared to the negative control group, APS (100mg/kg) and APS (200mg/kg) remarkably increased the expression of IFN-γ by 22.50±1.97% and 35.05±0.95%, respectively (Fig.8C). The levels of TNF-α and IFN-γ were significantly decreased in 5-FU group compared with those in negative control group (P<0.05). APS coupled to 5-Fu could recover the levels of TNF-α and IFN-γ that damaged by 5-Fu, suggesting the protective effect of APS on immune function in BALB/c mice. Besides, the results indicated that the anti-tumor effect of APS in 4T1-bearing mice might be associated with its ability to enhance the expression of TNF-α, IL-2 and IFN-γ.

3.5.5. Effects of APS on Bcl-2, Bax and caspase-3 proteins expression in tumor tissues

To further evaluate the mechanism of APS mediated apoptosis in tumor tissue, the protein expressions of Bax, Bcl-2 and caspase-3 were measured by immunohistochemical assay. As shown in Fig.9A, the proteins expression of Bax and caspase-3 increased, while the level of anti-apoptotic Bcl-2 in solid tumors decreased after treatment with APS and 5-FU. Besides, tumor cells were loosely arranged and nuclear fragmentations (orange arrows) were easily identified in 5-FU and combined group (Fig.9A). The results of semi-quantitative analysis of IHC demonstrated that APS (200 mg/kg) and 5-FU significantly down-regulated the proteins

16

expression of Bcl-2 compared with that in negative control group (P<0.01, Fig.9B). On the contrary, APS administration (100 and 200 mg/kg) markedly up-regulated the expression of Bax as compared to that in negative control group (P<0.05, P<0.01, Fig.9C). The expression of caspase-3 was significantly higher in APS (200 mg/kg) than that in negative control group (P<0.05, Fig.9D). APS combined with 5-FU led to a higher proteins expression of Bax and caspase-3 when compared with mice treated with APS or 5-FU alone.

4. Conclusion

In conclusion, the present study identified *in vitro* and *in vivo* antitumor activity of APS from the point of immunomodulatory mechanism. Although APS had no cytotoxicity towards 4T1 cells, APS could activate macrophages and further suppressed the growth of 4T1 cells by inducing cell apoptosis and arresting cell cycle in G2 phase. APS-treated macrophages promoted the apoptosis of breast cancer cells mainly through the mitochondrial apoptosis pathway. Anti-cancer activity *in vivo* of APS may be achieved by restoring immune organs, regulating cellular immune responses and increasing cytokine levels. APS combined with 5-FU could improve the anti-tumor effect and alleviate the damage of 5-FU on immune system, which is suitable as an immune adjuvant for chemotherapy.

Reference

[1] S.Y. Qin, Y.J. Cheng, Q. Lei, A.Q. Zhang, X.Z. Zhang, Combinational strategy for high-performance cancer chemotherapy, Biomaterials 171 (2018) 178-197.

[2] M.K. Patel, B. Tanna, H. Gupta, A. Mishra, B. Jha, Physicochemical, scavenging and anti-proliferative analyses of polysaccharides extracted from psyllium (Plantago ovata Forssk) husk and seeds, Int. J. Biol. Macromol. 133 (2019) 190-201.

[3] T. Khan, A. Date, H. Chawda, K. Patel, Polysaccharides as potential anticancer agents-A review of their progress, Carbohyd. Polym. 210 (2019) 412-428.

[4] L. Ren, C. Perera, Y. Hemar, Antitumor activity of mushroom polysaccharides: a review, Food Funct. 3(11) (2012) 1118-1130.

[5] J.H. Xie, W. Tang, M.L. Jin, J.E. Li, M.Y. Xie, Recent advances in bioactive polysaccharides from Lycium barbarum L., Zizyphus jujuba Mill, Plantago spp., and Morus spp.: Structures and functionalities, Food Hydrocolloid. 60 (2016) 148-160.

[6] N.V. Kladar, N.S. Gavarić, B.N. Božin, Ganoderma: insights into anticancer effects, Eur. J. Cancer Prev. 25(5) (2015) 462-471.

[7] J. Yu, H. Ji, X. Dong, Y. Feng, A. Liu, Apoptosis of human gastric carcinoma MGC-803 cells induced by a novel Astragalus membranaceus polysaccharide via intrinsic mitochondrial pathways, Int. J. Biol. Macromol. 126 (2019) 811-819.

[8] B. Yang, B. Xiao, T. Sun, Antitumor and immunomodulatory activity of Astragalus membranaceus polysaccharides in H22 tumor-bearing mice, Int. J. Biol. Macromol. 62(11) (2013) 287-290.

[9] L. Guo, S.P. Bai, L. Zhao, X.H. Wang, Astragalus polysaccharide injection integrated with vinorelbine and cisplatin for patients with advanced non-small cell lung cancer: effects on quality of life and survival, Med. Oncol. 29(3) (2012) 1656-1662.

[10] W. Li, K. Song, S. Wang, C. Zhang, M. Zhuang, Y. Wang, T. Liu, Anti-tumor potential of astragalus polysaccharides on breast cancer cell line mediated by macrophage activation, Mat. Sci. Eng. C-Mater. 98 (2019) 685-695.

[11] N. He, L. Tian, X. Zhai, X. Zhang, Y. Zhao, Composition characterization, antioxidant capacities and anti-proliferative effects of the polysaccharides isolated from Trametes lactinea (Berk.) Pat, Int. J. Biol. Macromol. 115 (2018) 114-123.

[12] B. Hu, T. Deng, H. Ma, Y. Liu, P. Feng, D. Wei, N. Ling, L. Li, S. Qiu, L. Zhang, B. Peng, J. Liu, M. Ye, Deubiquitinase DUB3 regulates cell cycle progression via stabilizing cyclin a for proliferation of non-small cell lung cancer cells, Cells 8(4) (2019) 297-310.

[13] B. P. Tian, F. Li, R. Li, X. Hu, T.W. Lai, J. Lu, Y. Zhao, Y. Du, Z. Liang, C. Zhu, W. Shao, W. Li, Z.H. Chen, X. Sun, X. Chen, S. Ying, D. Ling, H. Shen, Nanoformulated ABT-199 to effectively target Bcl-2 at mitochondrial membrane alleviates airway inflammation by inducing apoptosis, Biomaterials 192 (2019) 429-439.

[14] S. Su, J. Zhao, Y. Xing, X. Zhang, J. Liu, Q. Ouyang, J. Chen, F. Su, Q. Liu, E. Song, Immune checkpoint inhibition overcomes ADCP-induced immunosuppression by macrophages, Cell 175(2) (2018) 442-457.

[15] F. Kong, F.E. Li, Z. He, Y. Jiang, R. Hao, X. Sun, H. Tong, Anti-tumor and macrophage activation induced by alkali-extracted polysaccharide from Pleurotus ostreatus, Int. J. Biol. Macromol. 69(8) (2014) 561-566.

[16] H. Jin, Z. Ye, Z. Yuanyuan, F. Jia, Z. Weiping, I.O.L. Ng, S. Huichuan, Q. Lunxiu, Q. Shuangjian, J.M.F. Lee, Hepatic RIG-I predicts survival and interferon-α therapeutic response in hepatocellular carcinoma, Cancer Cell 25(1) (2014) 49-63.

[17] N. Chattopadhyay, T. Ghosh, S. Sinha, K. Chattopadhyay, P. Karmakar, B. Ray, Polysaccharides from Turbinaria conoides: Structural features and antioxidant capacity, Food Chem. 118(3) (2010) 823-829.

[18] N.J. Borazjani, M. Tabarsa, S. You, M. Rezaei, Purification, molecular properties, structural characterization, and immunomodulatory activities of water soluble polysaccharides from Sargassum angustifolium, Int. J. Biol. Macromol. 109 (2018) 793-802.

[19] W. Qiang, S. Xiaojing, S. Aimin, H. Hui, Y. Ying, L. Li, F. Ling, L. Hongzhi, β-Glucans: Relationships between modification, conformation and functional activities, Molecules 22(2) (2017) 257-269.

[20] V.E.C. Ooi, F. Liu, Immunomodulation and anti-cancer activity of polysaccharide-protein complexes, Curr. Med. Chem. 7(7) (2000) 715-729.

[21] U. Surayot, J. Wang, P. Seesuriyachan, A. Kuntiya, M. Tabarsa, Y.J. Lee, J.K. Kim, W.J. Park, S.G. You, Exopolysaccharides from lactic acid bacteria: Structural analysis, molecular weight effect on immunomodulation, Int. J. Biol. Macromol. 68(25) (2014) 233-240.

[22] W. Jiang, B.Y.S. Kim, J.T. Rutka, W.C.W. Chan, Nanoparticle-mediated cellular response is size-dependent, Nat. Nanotechnol. 3(3) (2008) 145-150.

[23] A. John, J. Yang, J. Liu, Y. Jiang, B. Yang, The structure changes of water-soluble polysaccharides in papaya during ripening, Int. J. Biol. Macromol. 115 (2018) 152-156.

[24] M. Lai, J. Wang, J. Tan, J. Luo, L.M. Zhang, D.Y.B. Deng, L. Yang, Preparation, complexation mechanism and properties of nano-complexes of Astragalus polysaccharide and amphiphilic chitosan derivatives, Carbohyd. Polym. 161 (2017) 261-269.

[25] M. Jin, K. Zhao, Q. Huang, P. Shang, Structural features and biological activities of the polysaccharides from Astragalus membranaceus, Int. J. Biol. Macromol. 64(2) (2014) 257-266.

[26] Z.Y. Zhu, R.Q. Liu, C.L. Si, Z. Fang, Y.X. Wang, L.N. Ding, J. Chen, A.J. Liu, Y.M. Zhang, Structural analysis and anti-tumor activity comparison of polysaccharides from Astragalus, Carbohyd. Polym. 85(4) (2011) 895-902.

[27] J.A. Kralovec, K.L. Metera, J.R. Kumar, L.V. Watson, G.S. Girouard, Y. Guan, R.I. Carr, C.J. Barrow, H.S. Ewart, Immunostimulatory principles from yrenoidosa—Part 1: Isolation and biological assessment in vitro, Phytomedicine 14(1) (2007) 57-64.

[28] C.M. Yang, Q.J. Han, K.L. Wang, Y.L. Xu, J.H. Lan, G.T. Cao, Astragalus and ginseng polysaccharides improve developmental, intestinal morphological, and immune functional Ccharacters of weaned piglets, Front. Physiol. 10 (2019) 418-428.

[29] C.H. Wang, C.Y. Lin, J.-S. Chen, C.L. Ho, K.M. Rau, J.T. Tsai, C.S. Chang, S.P. Yeh, C.F. Cheng, Y.L. Lai, Karnofsky performance status as a predictive factor for cancer-related fatigue treatment with Astragalus polysaccharides (PG2) injection-a double blind, multi-center, randomized phase IV study, Cancers 11(2) (2019) 128-140.

[30] Q.E. Tian, H.D. Li, M. Yan, H.L. Cai, Q.Y. Tan, W.Y. Zhang, Astragalus polysaccharides can regulate cytokine and P-glycoprotein expression in H22 tumor-bearing mice, World J. Gastroentero. 18(47) (2012) 7079-7086.

[31] J. Wang, Y.S. Zhang, K. Thakur, S.S. Hussain, J.G. Zhang, G.R. Xiao, Z.J. Wei, Licochalcone A from licorice root, an inhibitor of human hepatoma cell growth via induction of cell apoptosis and cell cycle arrest, Food Chem.Toxicol. 120 (2018) 407-417.

[32] C. Sawyers, Targeted cancer therapy, Nature 432(7015) (2004) 294-297.

[33] G.I. Evan, K.H. Vousden, Proliferation, cell cycle and apoptosis in cancer, Nature 411(6835) (2001) 342-348.

[34] J. Koff, S. Ramachandiran, L. Bernal-Mizrachi, A time to kill: Targeting apoptosis in cancer, Int. J.Mol. Sci. 16(2) (2015) 2942-2955.

[35] Y.Z. Wu, J. Sun, Y.B. Wang, Selective estrogen receptor modulator: A novel polysaccharide from Sparganii Rhizoma induces apoptosis in breast cancer cells, Carbohyd. Polym. 163 (2017) 199-207.

[36] Y. Wang, S. Wang, R. Song, J. Cai, J. Xu, X. Tang, N. Li, Ginger polysaccharides induced cell cycle arrest and apoptosis in human hepatocellular carcinoma HepG2 cells, Int. J. Biol. Macromol. 123 (2019) 81-90.

[37] C.M. Henry, E. Hollville, S.J. Martin, Measuring apoptosis by microscopy and flow cytometry, Curr. Protoc. Immunol. 61(2) (2013) 90-97.

[38] X. Liu, F. Liu, S. Zhao, B. Guo, P. Ling, G. Han, Z. Cui, Purification of an acidic polysaccharide from Suaeda salsa plant and its anti-tumor activity by activating mitochondrial pathway in MCF-7 cells, Carbohyd. Polym. 215 (2019) 99-107.

[39] G.M. Jose, M. Raghavankutty, G.M. Kurup, Sulfated polysaccharides from Padina tetrastromatica induce apoptosis in HeLa cells through ROS triggered mitochondrial pathway, Process Biochem. 68 (2018) 197-204.

[40] R. Youle, A. Strasser, The BCL-2 protein family: opposing activities that mediate cell death, Nat. Rev. Mol.Cell Bio. 9(1) (2008) 47-59.

[41] Y.L.P. Ow, D.R. Green, Z. Hao, T.W. Mak, Cytochrome c: functions beyond respiration, Nat. Rev. Mol.Cell Bio. 9(7) (2008) 532-542.

[42] L. Lin, K. Cheng, Z. Xie, C. Chen, L. Chen, Y. Huang, Z. Liang, Purification and characterization a polysaccharide from Hedyotis diffusa and its apoptosis inducing activity toward human lung cancer cell line A549, Int. J. Biol. Macromol. 122 (2019) 64-71.

[43] W. Wei, H.T. Xiao, W.R. Bao, D.L. Ma, C.H. Leung, X.Q. Han, C.H. Ko, B.S. Lau, C.K. Wong, K.P. Fung, TLR-4 may mediate signaling pathways of Astragalus polysaccharide RAP induced cytokine expression of RAW264.7 cells, J. Ethnopharmacol. 179(8) (2016) 243-252.

[44] J. Wu, J. Yu, W. Jing, C. Zhang, K. Shang, X. Yao, B. Cao, Astragalus polysaccharide enhanced antitumor effects of Apatinib in gastric cancer AGS cells by inhibiting AKT signalling pathway, Biomed. Pharmacother. 100 (2018) 176-183.

[45] S.S. Ferreira, C.P. Passos, P. Madureira, M. Vilanova, M.A. Coimbra, Structure-function relationships of immunostimulatory polysaccharides: A review, Carbohyd. Polym. 132 (2015) 378-396.

[46] G. Pang, F. Wang, L.W. Zhang, Dose matters: Direct killing or immunoregulatory effects of natural polysaccharides in cancer treatment, Carbohyd. Polym. 195 (2018) 243-256.

[47] G.H. Mao, Y. Ren, Q. Li, H.Y. Wu, D. Jin, T. Zhao, C.Q. Xu, D.H. Zhang, Q.D. Jia, Y.P. Bai, L.Q. Yang, X.Y. Wu, Anti-tumor and immunomodulatory activity of selenium (Se)-polysaccharide from Se-enriched Grifola frondosa, Int. J. Biol. Macromol. 82 (2016) 607-613.

[48] C. Lohmann, A. Muschaweckh, S. Kirschnek, L. Jennen, H. Wagner, G. Häcker, Induction of tumor cell apoptosis or necrosis by conditional expression of cell death proteins: analysis of cell death pathways and in vitro immune stimulatory potential, J. Immunol. 182(8) (2009) 4538-4546.

[49] C.Y. Ho, T.W.C. Lo, K.N. Leung, K.P. Fung, Y.M. Choy, The immunostimulating activities of anti-tumor polysaccharide from K1 capsular (polysaccharide) antigen isolated from Klebsiella pneumoniae, Immunopharmacology 46(1) (2000) 1-13.

[50] Y. Meng, Y. Zhang, N. Jia, H. Qiao, M. Zhu, Q. Meng, Q. Lu, Y. Zu, Synthesis and evaluation of a novel water-soluble high Se-enriched Astragalus polysaccharide nanoparticles, Int. J. Biol. Macromol. 118 (2018) 1438-1448.

[51] S. Fan, G. Yu, W. Nie, J. Jin, L. Chen, X. Chen, Antitumor activity and underlying mechanism of Sargassum fusiforme polysaccharides in CNE-bearing mice, Int. J. Biol. Macromol. 112 (2018) 516-522.

[52] G. Pang, S. Zhang, X. Zhou, H. Yu, Y. Wu, T. Jiang, X. Zhang, F. Wang, Y. Wang, L.W. Zhang, Immunoactive polysaccharide functionalized gold nanocomposites promote dendritic cell stimulation and antitumor effects, Nanomedicine 14(10) (2019) 1291-1306.

[53] U.J. Yun, S.E. Park, Y.S. Jo, J. Kim, D.Y. Shin, DNA damage induces the IL-6/STAT3 signaling pathway, which has anti-senescence and growth-promoting functions in human tumors, Cancer Lett. 323(2) (2012) 155-160.

[54] X. Sun, R.L. Gao, Y.K. Xiong, Q.C. Huang, M. Xu, Antitumor and immunomodulatory effects of a water-soluble polysaccharide from Lilii Bulbus in mice, Carbohyd. Polym. 102(1) (2014) 543-549.

[55] D. Mumberg, P.A. Monach, S. Wanderling, M. Philip, A.Y. Toledano, R.D. Schreiber, H. Schreiber, CD4+ T cells eliminate MHC class II-negative cancer cells in vivo by indirect effects of IFN-?, P. Natl. Acad. Sci. USA 96(15) (1999) 8633-8638.

Figure legends

Fig.1. Structure and composition of APS. (A) Macroscopical appearance of APS. (B) ^{1}H-NMR and ^{13}C-NMR spectra of APS. (C) HPLC chromatogram of derivative APS.

Fig.2. Effect of CM on the growth of 4T1 cells. (A) Live/dead staining to evaluate the effect of CM on the viability of 4T1 cells after incubation for 48h. Scale: 100μm. (B) The inhibitory rate of 4T1 cells cultured with different dosages of APS-mediated CM were evaluated by CCK-8 assay after incubation for 24, 48, and 72 h, respectively, (n = 4). (C) Cell cycle distribution by flow cytometry of 4T1 cells in the presence of CM mediated by various concentrations of APS and 5-FU for 48h, respectively. (D) Cell cycle profile of 4T1 cells after exposure to CM for 48 h, respectively. * P<0.05, ** P<0.01 vs. negative control group. *** P<0.001 compared between CM groups and negative control group; $^{\#\#}$ P<0.01, $^{\#\#\#}$ P<0.001 compared between 5-FU and APS mediated CM at a concentration of 1000 μg/mL.

Fig.3. APS mediated CM induced the apoptosis of 4T1cells. (A) Nuclear condensations of 4T1 cells were visualized under a fluorescent microscope after exposure to CM and 5-FU. Condensed nuclei and the apoptotic bodies are indicated by green arrows. Scale bar=50 μm. (B)
Flow cytometry analysis of apoptosis induced by CM in 4T1 cells using Annexin V-FITC staining. (C) The percentage of apoptotic 4T1 cells with the intervention of CM. **P<0.01, vs. negative control group. $^{\#}$P<0.05, $^{\#\#}$P<0.01, compared between 5-FU and APS mediated CM at a concentration of 1000 μg/mL. (D) SEM observation of 4T1 cell morphology after exposure to CM and 5-FU, respectively. Magnification of the images was 3,000× and 10,000× (green border). Scale bar=20 μm.

Fig.4. CM induced the apoptotis of 4T1 cells by mitochondria pathway. (A) Immunofluorescent pictures of Bcl-2 and Bax of 4T1 cells after exposure to APS mediated CM and 5-FU, respectively. Scale bar=30 μm. (B) Bcl-2 and Bax protein expression in 4T1 cells by flow cytometry intracellular staining. (C) The ratio of Bax and Bcl-2 protein expression in MCF-7 and 4T1 cells. (D) CM mediated the release of cytochrome c in 4T1 cells. (E) CM induced the activation of caspase-9 and caspase-3 in 4T1 cells. * P<0.05, ** P<0.01, CM groups vs. negative control group (untreated cells). $^{\#}$ P<0.05, compared between 5-FU and APS mediated CM at a concentration of 1000 μg/mL.

Fig.5. Effect of APS on the tumor growth in BALB/c mice. (A) The changes of tumor sizes during the 14 days of administration in all groups. *P<0.05, **P<0.01, ***P<0.001, other groups vs. negative control group. $^{\#}$P<0.05, $^{\#\#}$P<0.01, $^{\#\#\#}$P<0.001, other groups vs. 5-FU group. (B)

Macroscopic presentation of tumor after intragastric injection for 14 days. (C) Effect of APS on microstructure of tumor tissue. Scale bar=100μm.

Fig.6. Effect of APS on the morphologic structure of thymus (A) and spleen (B). Scale bar = 100μm.

Fig.7. Effect of APS on phagocytosis of macrophages and the proliferation of lymphocytes. (A) Phagocytosis index of peritoneal macrophage after treatment with APS. (B) Effect of APS on the proliferation of spleen lymphocytes. The percentage of normal group was calculated as 100%. *P<0.05, vs. negative control group. △P<0.05, △△P<0.01, compared with normal control group. **P<0.01, ***P<0.001, compared with negative control group. #P<0.05, ###P<0.001, compared with 5-FU group.

Fig.8. Effects of APS on the production of serum cytokines in mice. (A-C) Effect of APS on the expression of TNF-α, IL-2 and IFN-γ, respectively. *P<0.05, compared with negative control group. ##P<0.01, compared with 5-FU group.

Fig.9. Effects of APS on the expression of apoptotic-related protein in tumor tissue. (A) The protein expression of Bcl-2, Bax and caspase-3 in all groups. Scale bar=50μm. (B-D) Mean density of Bcl-2, Bax and caspase-3 in all groups using IPP software, respectively. *P<0.05, *P<0.01, compared between APS group and negative control group.
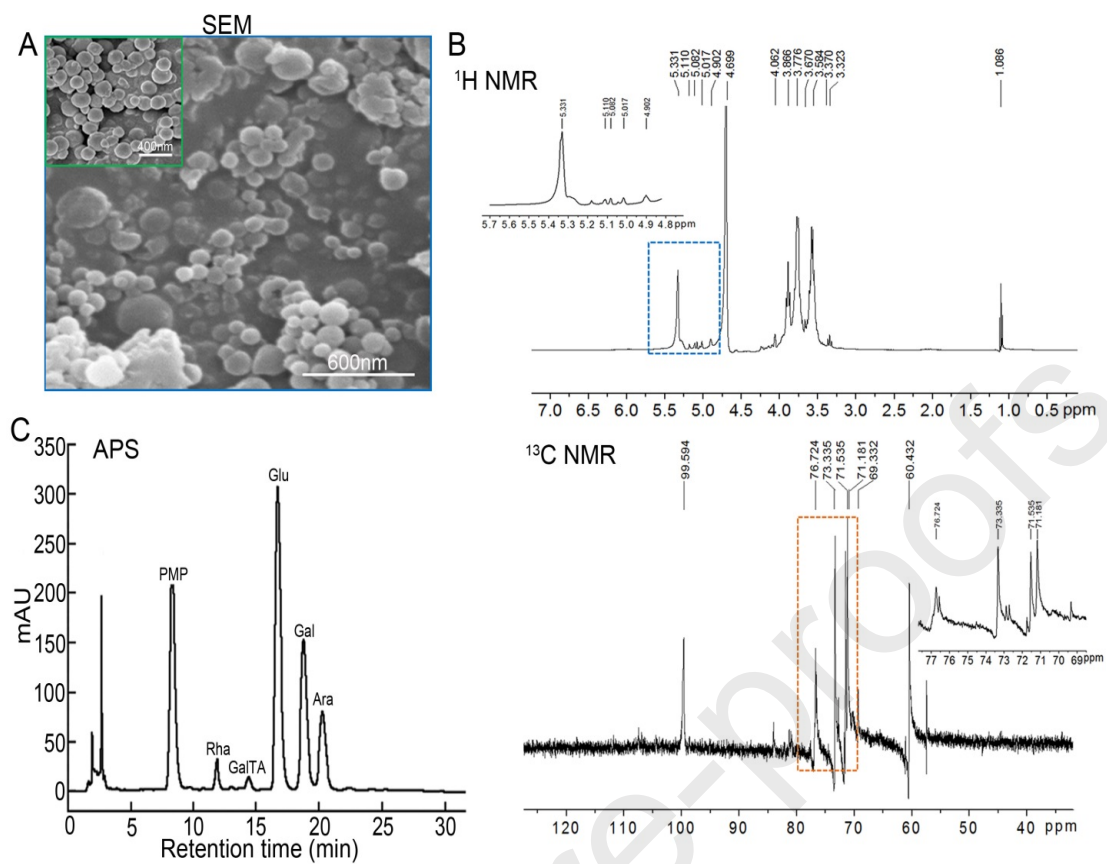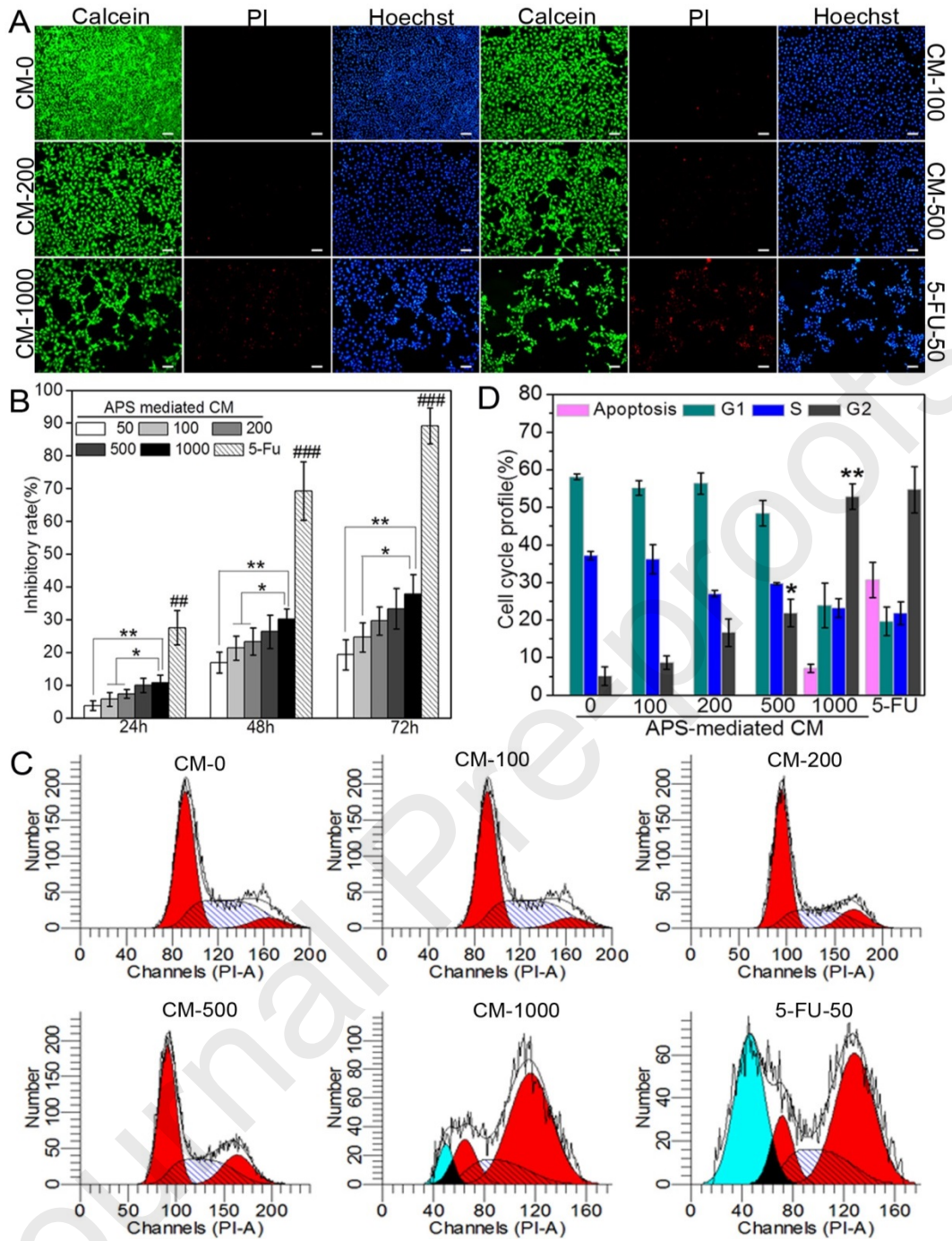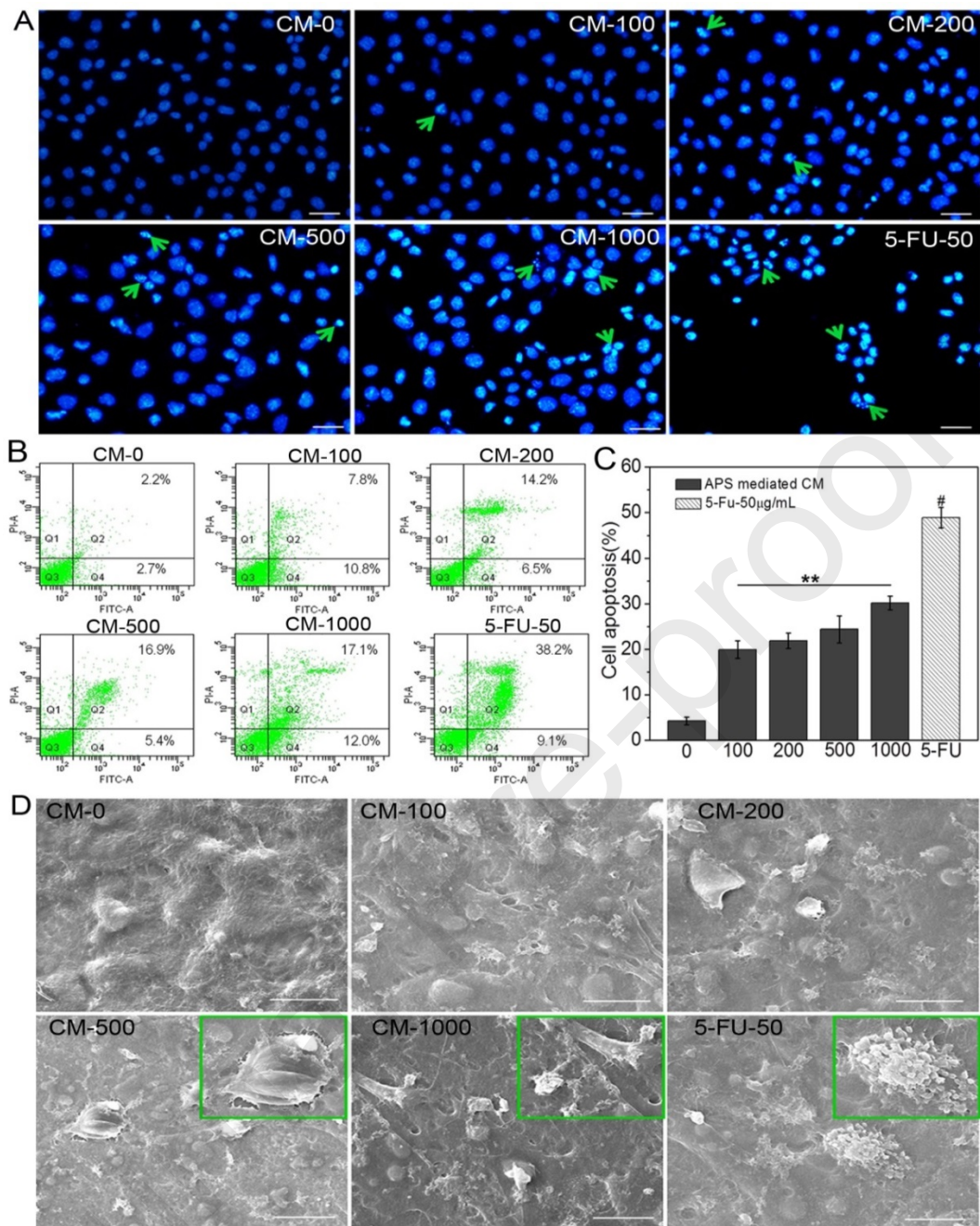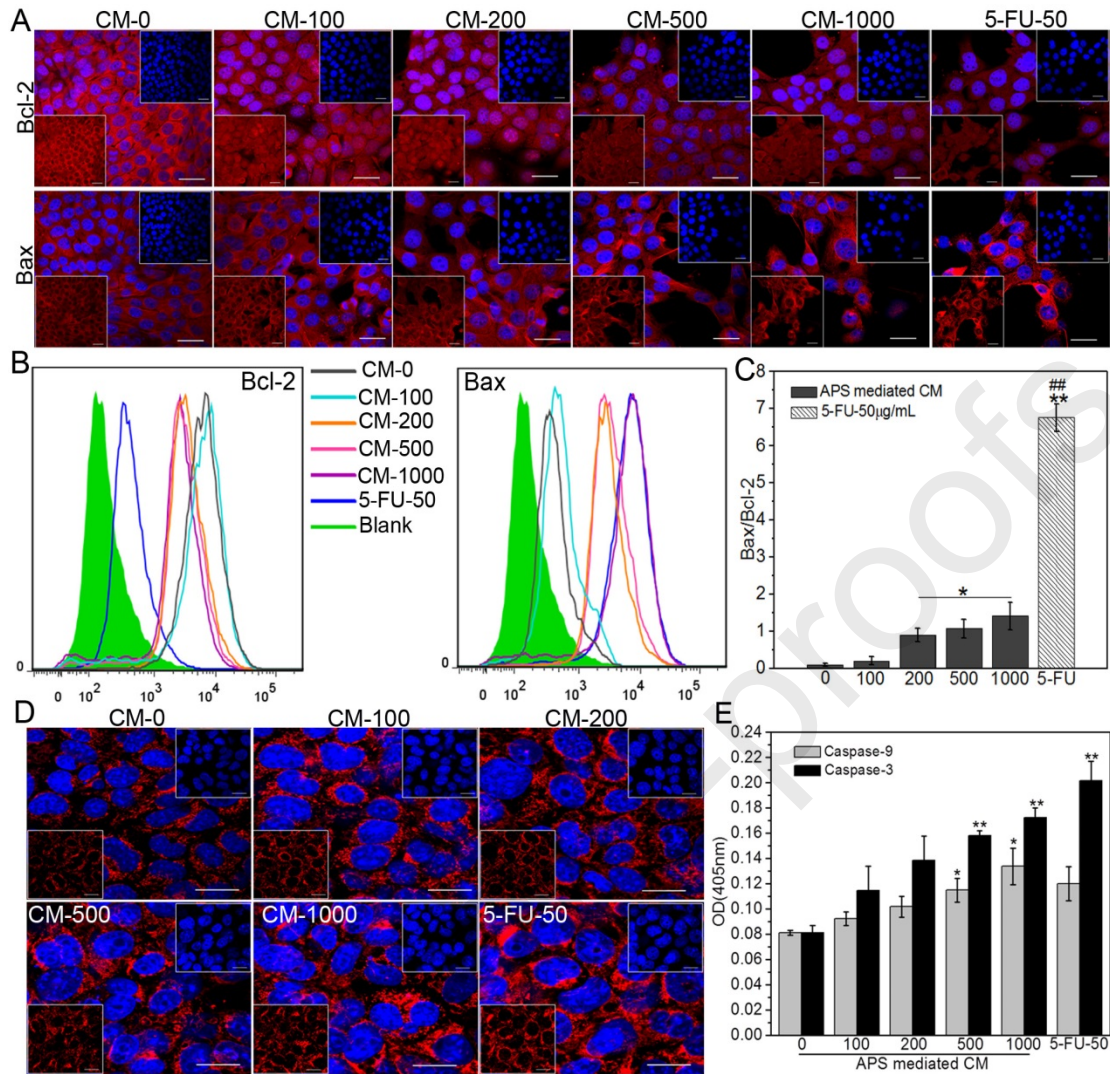
Fig.1

Fig.2

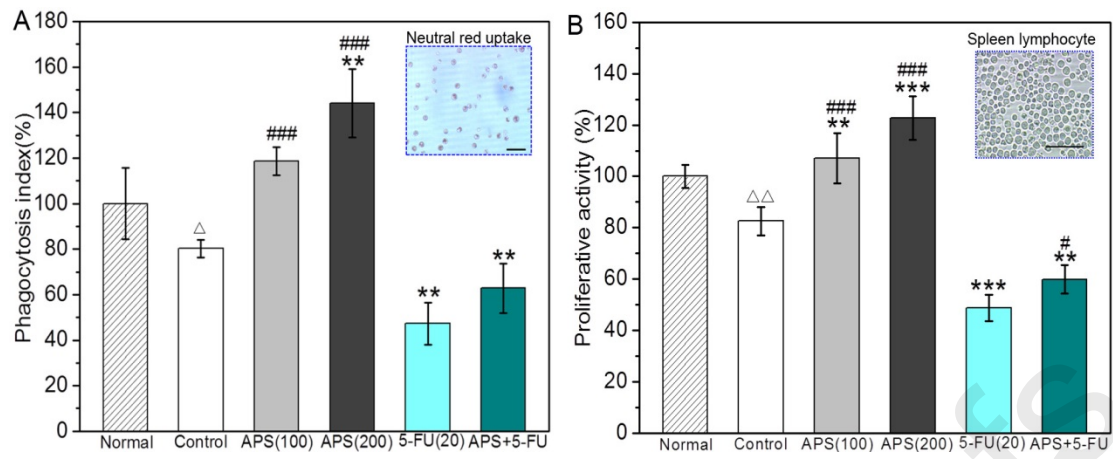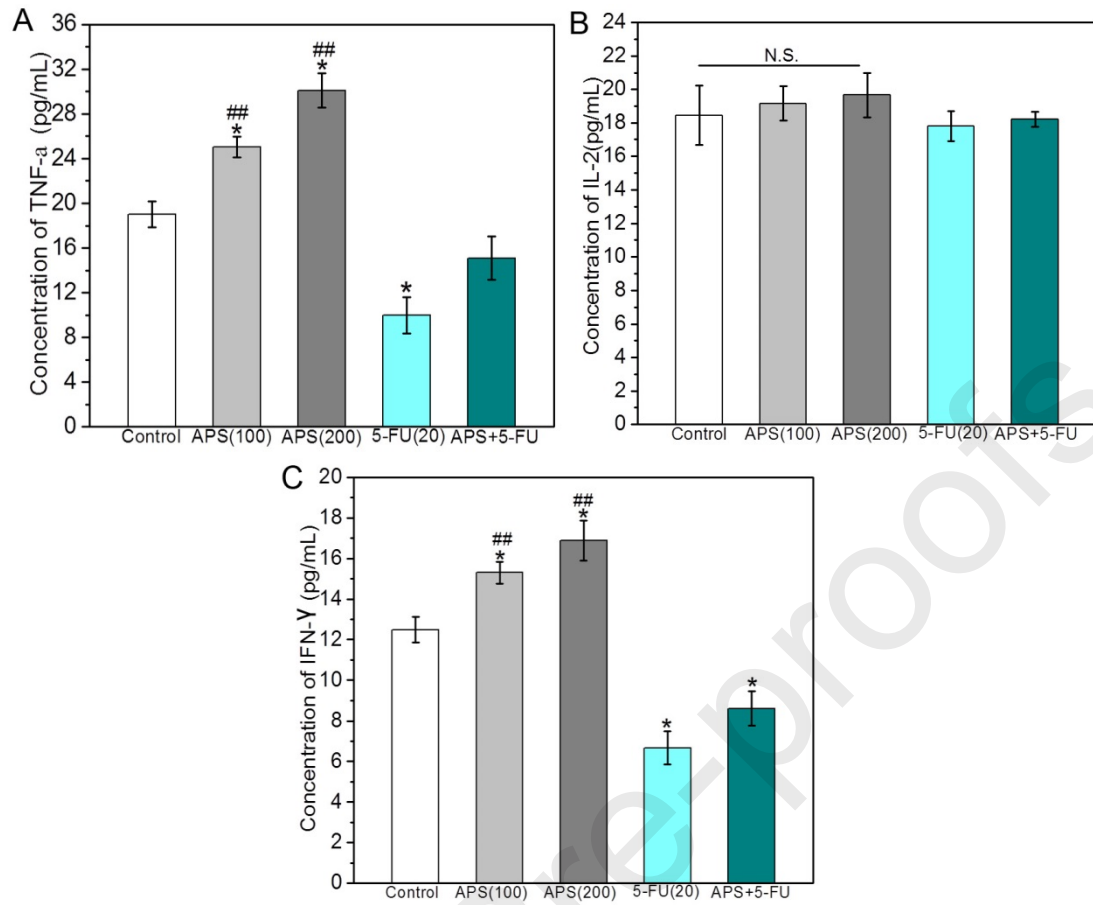**Fig.3**

Fig.4
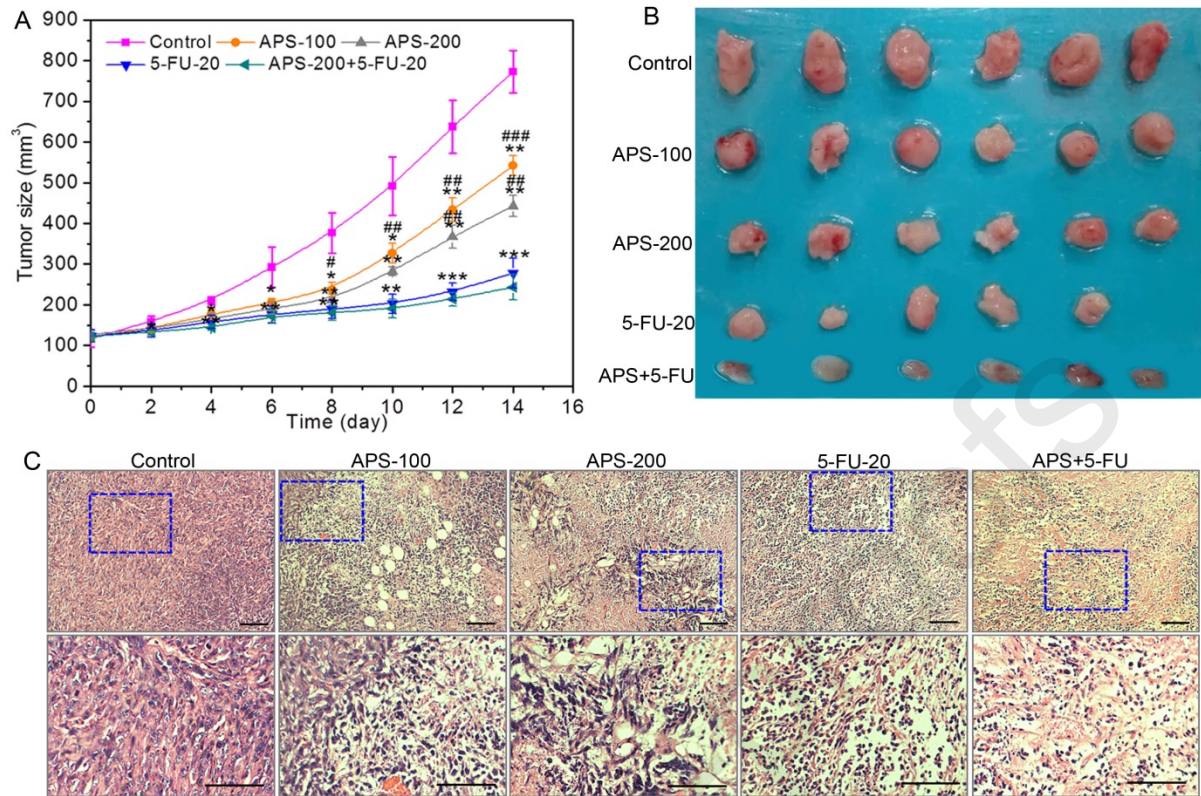
Fig.5
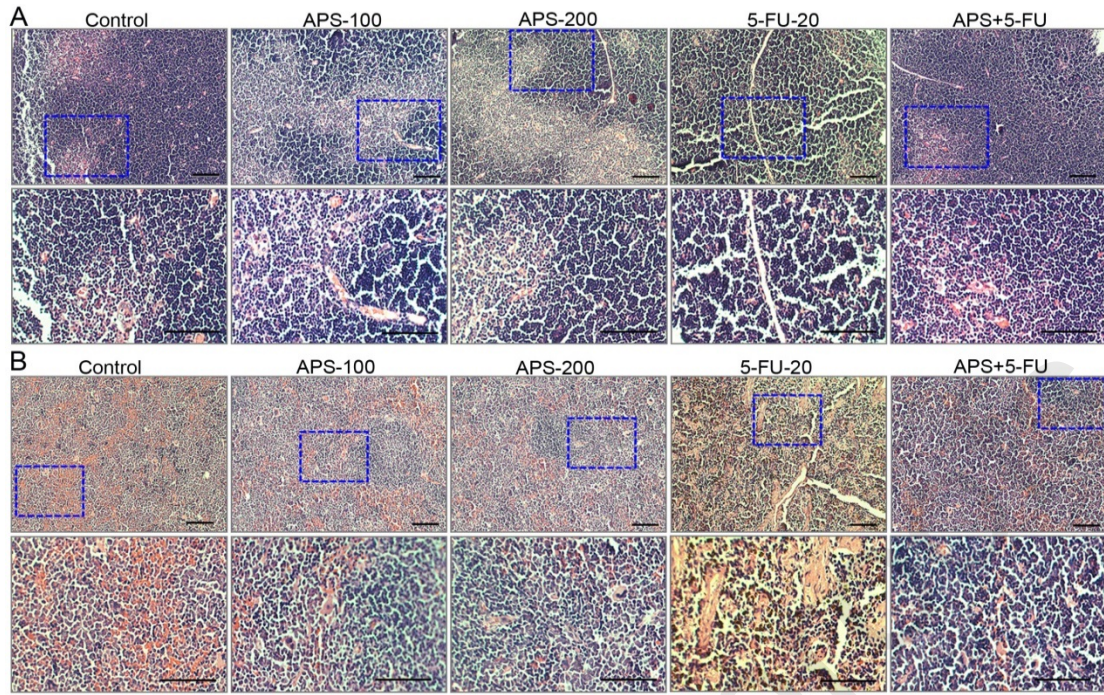
Fig.6

Fig.7

Fig.8

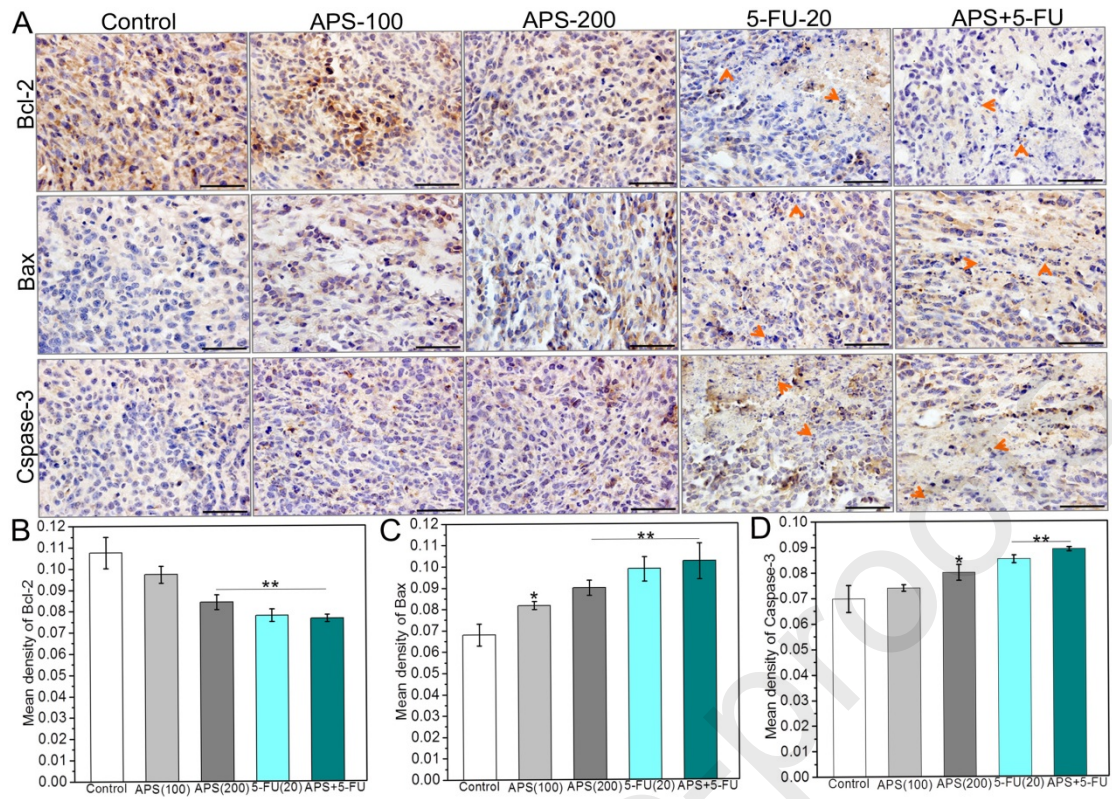**Fig.9**

Tab.1 Effect of APS on tumor growth of BALB/c mice. *P<0.05, **P<0.01, ***P<0.001, compared with negative control group. $^{\#}$P<0.05, $^{\#\#}$P<0.01, compared with 5-FU group.

Group	Dosage(mg/kg)	Tumor weight(g)	Inhibitory rate (%)
Negative control	-	0.188±0.0179	-
APS-1	100	0.158±0.0138$^{*\#\#}$	16.19±0.77$^{\#\#\#}$
APS-2	200	0.139±0.0204$^{**\#}$	26.43±5.50$^{\#\#}$
5-FU	20	0.107±0.0135***	43.26±5.59
APS-2+5-FU	APS(200)+5-FU(20)	0.0907±0.0142***	51.81±5.26

Tab.2 Effect of APS on the thymus index and spleen index in BALB/c mice. *P<0.05, **P<0.01, compared with negative control group. $^{#}$P<0.05, $^{##}$P<0.01, $^{###}$P<0.001, compared with 5-FU group.

Group	Dosage(mg/kg)	Spleen index(mg/g)	Thymus index(mg/g)
Negative control	-	5.33±0.43	1.23±0.41
APS-1	100	6.27±0.76$^{##}$	1.52±0.18$^{###}$
APS-2	200	7.13±0.63$^{**###}$	1.79±0.15$^{*###}$
5-FU	20	3.67±0.59**	0.72±0.12*
APS-2+5-FU	APS(200)+5-FU(20)	4.46±0.42*	0.91±0.19

Highlights:

1. APS was non-cytotoxic against 4T1 cells

2. APS mediated macrophages inhibited the growth of 4T1 cells

3. APS mediated macrophages induced cell apoptosis by mitochondrial pathway

4. APS exhibited *in vivo* anti-tumor activity by immunoregulation

5. APS alleviated immunosuppression of 5-FU on immune system

Graphic abstract

Astragalus polysaccharide (APS) has attracted growing interests in the field of anti-cancer by direct killing effect and improving immune function. In this study, the structure and composition of APS was determined, following the evaluation of *in vitro* and *in vivo* anti-tumor activity of APS targeted macrophages and host immune system based on immunoregulated strategy. The results indicated that APS had no direct cytotoxicity against 4T1 cells, but APS mediated macrophages could significantly inhibit the growth of 4T1 cells by the induction of cell cycle arrest (G2 phase) and cell apoptosis. APS mediated macrophages promoted the apoptosis of 4T1 cells mainly through the mitochondrial apoptosis pathway. The *in vivo* findings demonstrated that APS could markedly improve the thymus index and spleen index, and restore the structure of the damaged thymus and spleen tissue. APS could significantly enhance the proliferation of spleen lymphocytes and increase phagocytosis of peritoneal macrophages in mice. Furthermore, APS was capable of up-regulating the expression of IL-2, TNF-α and IFN-γ in peripheral blood. APS combined with 5-FU could improve the anti-tumor effect accompanied by the immunosuppressive alleviation of 5-FU on immune system, which may be suitable as an immune adjuvant for chemotherapy.

APS exhibited *in vitro* and *in vivo* anti-tumor activity targeted macrophages and host immune system via immunoregulation